Efficient Simulation of the Impulse Response of the Indoor Wireless Optical Channel

Cipriano R. Lomba[†], Rui T. Valadas, A. M. de Oliveira Duarte
University of Aveiro, 3800 Aveiro, Portugal
Fax: +351 234381941 Email: cipriano.lomba@ent.efacec.pt

Abstract

The use of wireless local area networks (WLANs) is experiencing a significant growth. Infrared technology has an extensive bandwidth of free use, and has the potential to be the support of high-baud rate WLANs. For that, it is necessary to understand the propagation characteristics of the indoor optical channel. This paper presents a computationally efficient algorithm for the simulation of indoor optical channels, considering multiple reflections of the emitted signal. The models used to approximate the emitter pattern, the propagation environment and the receiver pattern are described. Two new procedures (called *Time Delay Agglutination* and *Time and Space Indexed Tables*) are introduced to increase the efficiency of the simulation of the impulse response of the indoor wireless optical channel. The structure of the algorithm is presented and the approaches used are discussed. The new algorithm was implemented in a simulation package, named SCOPE, which is very efficient and allows to evaluate the main parameters of indoor optical channels considering multiple reflections of the emitted signal. Results obtained for several channels are compared with experimental and published values, and good agreement is verified.

Keywords: Optical wireless, Optical channel simulation, IR indoor systems, Simulation methods.

1 Introduction

Over the last decade, the use of wireless local area networks (WLAN) has verified a substantial growth. Current WLANs have baud rates limited to a few Mbps. However, to guaranty future success of WLANs it is necessary to increase their baud rates up to, at least, 10 Mbps. Infrared (IR) technology offers an extensive bandwidth that is of free use, and has the potential to become the support of high baud rate WLANs.[1–4] The performance of IR communication systems can be affected by several factors, namely: (i) intense ambient noise,[5] (ii) large and variable propagation losses and (iii) multipath propagation, which may originate strong inter-symbol interference (ISI) for bit rates higher than about

[†]The author is currently at the R&D Direction of ENT Empresa Nacional de Telecomunicações, SA, Maia, Portugal, and would like to thanks JNICT for its financial support through a Ph. D. Grant – BD/1682/91-IA.

10 Mbps. The development of high-bit rate IR systems requires a detailed knowledge of the channel impulse response, which may be obtained following one of 3 different approaches: analytical modelling, experimental data or computer simulation. Simulation seems to be the most convenient, since analytical modelling of the signal propagation is too complex when considering multiple reflections, and experimental measurement of the impulse response is an expensive and lengthy task, as it has to be done on a channel-by-channel basis.

The first method to simulate the impulse response of indoor optical channels considering multiple reflections of the emitted signal was based on a simple recursive algorithm proposed by Barry *et al.*[6] However, the computing time increases rapidly with the number of reflections, and becomes too large when more than 2 reflections are considered. Several other research groups have studied the simulation of the indoor wireless optical channel.[3,4,7,8] This paper presents a new computationally efficient algorithm to evaluate the impulse response of indoor wireless optical channels, considering multiple reflections of the emitted signal. In Section 2, we review the models used to approximate emitter and receiver optical patterns, and describe three signal propagation models: the free-space propagation model, the single-reflection propagation model and the multiple-reflections propagation model, which can be used to approximate line-of-sight, quasi-diffuse and diffuse propagation environments, respectively. In Section 3, we introduce two new procedures that allow to increase the efficiency of the simulation process with the number of reflections considered. The main structure of the algorithm implemented in a simulator of the indoor optical channel, named SCOPE, is also described. In Section 4, we present results showing the time efficiency and performance of the SCOPE simulator in obtaining impulse responses of indoor optical channels. Finally, in Section 5, we present the main conclusions.

2 Indoor Optical Channel Modelling

In closed spaces, optical signals may propagate from emitter to receiver through multiple paths, due to reflections on surrounding surfaces and existing objects. The reflection pattern of most surfaces can be correctly approximated using the model of Lambert or the model of Phong.[9] The propagation characteristics of the indoor channel depend on the relative positioning of emitter, receiver and reflectors and their optical patterns. Movement of people or objects originate changes in those characteristics. Those changes are slow compared with the transmission bit rate, allowing to consider the channel stationary for specific positioning of emitter and receiver. Under this assumption, the channel impulse response $h(t)$ describes the propagation of the optical signal between emitter and receiver.

In general, indoor IR systems use short wavelength LEDs emitters and large area detectors. The angular distribution of the emitter radiant intensity is modelled using the *lambertian* law[3]

$$E(\phi) = \begin{cases} \frac{n+1}{2\pi} P_t \cos^n(\phi) & \text{for } \phi < \pi/2 \\ 0 & \text{for } \phi \geq \pi/2 \end{cases} \tag{1}$$

where P_t is the total emitted power, ϕ is the angle with the normal to the emitter surface and $n = -0.693/\ln[\cos(hpa)]$, being hpa the half-power angle of the emitter pattern. Emitter positioning is specified by the following set of parameters $\mathcal{E}= \{\vec{s}; \hat{n}_s; P_t, hpa\}$, where $\vec{s}$ and $\hat{n}_s$ represent the position and the orientation of the emitter.

The detector is modelled as an active area, A_D, collecting the radiation incident at angles θ smaller than the detector field-of-view (fov). Detector model is given by

$$D(\theta, fov) = \begin{cases} A_D \cos(\theta) & \text{for } \theta \leq fov \\ 0 & \text{for } \theta > fov \end{cases} \tag{2}$$

Detector positioning can be specified by the following set of parameters $\mathcal{D}= \{\vec{d}; \hat{n}_d; A_D, fov\}$, where $\vec{d}$ represents the position and $\hat{n}_d$ the orientation of the detector.

2.1 Signal Propagation Models

Depending on the reflection characteristics of the surfaces that surround the communication environment and on the application in view, indoor wireless IR systems may use different configurations. To take into account the system configuration, three models to approximate the propagation of optical signals in indoor spaces will be described.

2.1.1 Free-Space Propagation Model

In indoor systems, signals propagate over relatively short distances and attenuation due to absorption and scattering is minimum. Line-of-sight impulse response characterises the signal free-space propagation and is modelled by

$$h_0(t; \mathcal{E}, \mathcal{D})= \frac{m+1}{2\pi} \cos^m(\phi) \frac{A_D \cos(\theta)}{d_{ER}^2} \cdot \delta(t - \frac{d_{ER}}{c}) \tag{3}$$

where ϕ and θ are the emitting and the incidence angles, as defined previously, d_{ER} is the distance between emitter and receiver and $\delta(t - \frac{d_{ER}}{c})$ represents the signal propagation delay, where $\delta(t)$ is the Dirac function and c is the speed of light. This expression assumes that $\phi < 90°$ and $\theta < fov$ and is valid for $d_{ER} \gg \sqrt{A_D}$, which is in general verified.

2.1.2 Single–Reflection Propagation Model

When the ceiling is the only surface that reflects properly IR radiation, a quasi-diffuse system configuration can be used. Figure 1 illustrates the geometry considered to obtain the single-reflection propagation model. To model this propagation environment, the ceiling surface is considered to be divided into a large set of small areas, named *reflector elements*. Those areas are first considered collecting elements, and temporal and spatial distributions of the emitted signal over the ceiling are evaluated. Each element is then considered a point source that re-emits the collected signal scaled by the surface reflection coefficient. The channel impulse response after one reflection in the ceiling surface can be approximated by[3]

$$h_1(t; \mathcal{E}, \mathcal{D})= \sum_{j=1}^{M} \frac{(m+1) A_D \Delta A}{2\pi d_{Ej}^2 d_{jR}^2} \cos^m(\phi_{Ej}) \cos(\theta_j) R(\theta_j, \phi_j, S) \cos(\theta_{jR}) \cdot \delta(t - \frac{d_{Ej} + d_{jR}}{c}) \tag{4}$$

where M is the number of reflector elements in the fov of the detector, ϕ_{Ej} and θ_j are the emitting and the incidence angles and d_{Ej} is the distance between source and element j with area $\Delta A = \Delta s \times \Delta s$, being Δs the *spatial resolution*. $R(\theta_j, \phi_j, S)$ represents the surface

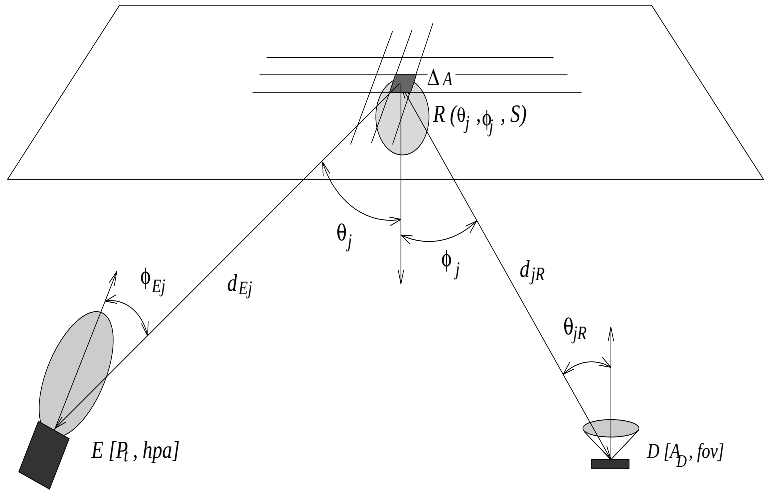

Figure 1: Geometry used to describe the single-reflection propagation model.

reflection pattern and it is assumed that $P_t = 1$. This equation is valid when $d_{jR} \gg \sqrt{A_D}$ and results accuracy increases with the spatial resolution used.

2.1.3 Multiple–Reflections Propagation Model

In many closed spaces, the surrounding surfaces reflect quite well IR signals, and a diffuse configuration system can be used. The emitted signal is successively reflected, before being collected by the detector, or absorbed by the room surfaces. Figure 2 illustrates this propagation scenario. Consider the reflecting surfaces divided in small reflecting elements of area

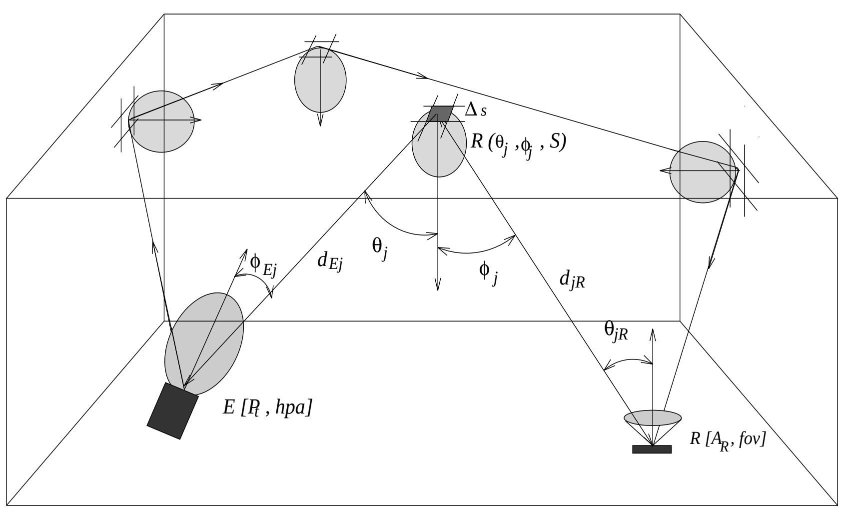

Figure 2: Geometry of reference for the multiple–reflections propagation model.

ΔA. As a detector, each element is defined by $\mathcal{D}_j$=$\{\vec{s_j}; \hat{n}_j; \Delta A, 90°\}$, where $\vec{s_j}$ is the position vector of reflector j that has area ΔA and $fov = 90°$ and $\hat{n}_j$ is the unitary vector normal to the reflector. As an emitter, each element is defined by $\mathcal{E}_j$= $\{\vec{s_j}; \hat{n}_j; P_j, R_j(\theta_i, \theta_o)\}$, where $\vec{s_j}$ and $\hat{n}_j$ are defined as previously, P_j is the power incident on the element j and $R_j(\theta_i, \theta_o)$ represents the surface reflection pattern. The signal time dispersion is modelled considering the delay in each propagation path between emitter and detector. The impulse response of this diffuse channel can be approximated by

$$h(t;\mathcal{E},\mathcal{D})= \sum_{k=0}^{\infty} h_k(t;\mathcal{E},\mathcal{D}) \tag{5}$$

where $h_k(t;\mathcal{E},\mathcal{D})$ is the *partial response of order* k, corresponding to the signal that suffers exactly k reflections before it goes into the detector and t is the total signal propagation delay. To evaluate $h_k(t;\mathcal{E},\mathcal{D})$ for $k>0$, Barry*et al.*[6] proposed a recursive algorithm where $h_k(t;\mathcal{E},\mathcal{D})$ is given by

$$h_k(t;\mathcal{E},\mathcal{D})= \frac{m+1}{2\pi} \sum_{j=1}^{M} \rho_j \cos^m(\phi_j) \frac{D(\theta_j,90°)}{d_{Ej}^2} h_{k-1}(t-d_{Ej}/c;\mathcal{E}_j,\mathcal{D})\ \Delta A \tag{6}$$

where M is the total number of reflector elements in the room, ρ_j is the reflection coefficient of j, d_{Ej} represents the distance from $\mathcal{E}$ to j and $h_{k-1}(t;\mathcal{E}_j,\mathcal{D})$ is the impulse response of order $k-1$ between reflector j and $\mathcal{D}$.

3 The SCOPE Simulator

Using the models presented above, we implemented the SCOPE simulator[10,11] that allows to evaluate the impulse response of indoor optical channels considering multiple reflections of the emitted signal. The obtained impulse response is given by a large set of Dirac pulses, which result from considering the reflecting surfaces divided in small areas that re-emit the incident signal as point sources. The line-of-sight impulse response from reflector i to reflector j is a Dirac function scaled by the path propagation gain $dP(i,j)$ and delayed by the signal propagation delay $\tau(i,j)$. Direct implementation of the recursive approach described previously is not time efficient for $k>2$, as it requires the evaluation of approximately M^k line-of-sight responses, where only M^2 are different. In a room with $10 \times 10 \times 4$ (m) and considering $\Delta s = 40$ cm, evaluation of $h_4(t;\mathcal{E},\mathcal{D})$ requires the computation of $M^k = 2.56 \times 10^{13}$ line-of-sight impulse responses. If each of those responses requires 1 μs to be evaluated, it will be necessary about 297 days to obtain the channel impulse response, making the simulation process not practical when considering more than 3 reflections. To reduce this increase in simulation time with the number of reflections, a new simulation algorithm was developed implementing the following approaches:

Time Delay Agglutination - Considering the optical source emits one Dirac pulse, all reflectors in line-of-sight with the source will collect a single optical pulse. After the first reflection, the number of pulses incident in each reflector equals the number of reflectors in line-of-sight with the source and, simultaneously, with that reflector. The number of pulses and signal dispersion increases rapidly for higher order reflections. To reduce this increase, the propagation delay at each reflector can be divided in uniform intervals Δt and all pulses with delays within each interval added, resulting in a single pulse with the average delay of the interval. This approach reduces the growth with k of the number of line-of-sight responses to be evaluated. The value considered for Δt may affect the impulse response obtained, but a set of simulations showed that using $\Delta t \approx \Delta s/c$ results in small errors and reduces considerably the simulation time.[3] Within each Δt, pulses are added independently of the incidence angle and re-emitted as a single pulse. Thus the model of Phong can not be used, as it depends on the incidence angle. However, in most environments the first reflection spreads the signal over the room surfaces, reducing the importance of the reflection model used. SCOPE allows the selection of the most appropriate reflection model to evaluate the first reflection, but for higher reflections the model of Lambert is used.

Space and Time Indexed Tables - In the SCOPE simulator the signal distribution (space and time) resulting from each reflection is evaluated at once. This allows the use of space and time indexed tables in fast memory, implementing the time agglutination approach in a very efficient way. In those tables, each line corresponds to a reflector element and each column to a given delay interval Δt of the agglutination process. Thus, when evaluating each signal reflection order, each table position stores the sum of all pulses arriving at one reflector within the corresponding time delay interval.

Progressively Decreased Resolution - Simulation time grows rapidly with the number of elementary areas. To reduce the SCOPE simulation time, Δs increases progressively with k. Moreover, line-of-sight signal distribution is evaluated using a value of Δs equal to half that defined by the user. The power collected at each reflector is the sum of that incident in the four smaller reflectors it contains, and delay equals the average delay of the four pulses. This approach increases the accuracy of the first reflection results without increasing overall simulation time. SCOPE was developed in C code and the main structure of the algorithm implemented is the following:

BEGIN
    Get input parameters and evaluate $h_0(t)$
    IF $(N = 0)$ { Store $h(t) = h_0(t)$ and show specified output results }
    ELSE {
        Evaluate power distribution and form factors, and build lookup tables
        Evaluate $h_1(t)$
        IF $(N = 1)$ { Store $h(t) = h_0(t) + h_1(t)$ and show specified output results }
        ELSE {
            $h(t) = h_0(t) + h_1(t)$
            FOR $k = 2$ TO N {
                IF $(\Delta s_k \neq \Delta s_{k-1})$ { Evaluate new form factors and build lookup tables }
                Evaluate signal distribution resulting from reflection $k - 1$
                Evaluate $h_k(t)$
                $h(t) = h(t) + h_k(t)$ }
            Store $h(t) = \sum_{k=0}^{N} h_k(t)$, evaluate and show specified output results }
        }
END

where $h_k(t)$ is a simplified notation for $h_k(t; \mathcal{E}, \mathcal{D})$, N is the number of reflections to consider and Δs_k is the spatial resolution used to evaluate $h_k(t)$. This approach is quite different from the recursive algorithm since computation of $h_k(t)$ is performed after $h_{k-1}(t)$ has been obtained and uses most of the calculations done to evaluate lower order partial responses. The *Time and Space Indexed Tables* procedure is used in the computation of every $h_k(t)$

($k > 0$) and to obtain the signal distribution after each reflection, while the *Time Delay Agglutination* approach is only used in the last one. The *Progressive Decreased Resolution* procedure is employed in the evaluation of the signal distribution after every reflection. Together, these procedures result in a significant reduction in the increase of the computation time with the number of reflections considered.

SCOPE allows to evaluate the main characteristics of the indoor optical channel in empty rooms. When starting each simulation, the user selects the output variables, namely, channel impulse response, channel transfer function, total collected power, collected power due to each reflection, channel propagation losses and average delay and root mean delay of the collected signal. With some user interaction, SCOPE allows to optimise the emitter pattern to minimise the maximum propagation losses over a specific cell configuration.

4 Simulation Results

To validate the results of SCOPE we followed two approaches: (i) results obtained for the optical power distribution in some closed spaces were compared with experimental data measured in those rooms and (ii) results obtained for the impulse response of specific channels were compared with results published by others researchers.[6,12]

4.1 Optical Power Distribution

We considered a diffuse system operating in a laboratory of the University of Aveiro. Table 1 resumes the room characteristics and simulation parameters.

Parameter	Value
Room dimensions (x, y, z)	$8.8 \times 7.0 \times 3.1$ (m)
$\rho_{ceiling}$, ρ_{North}, ρ_{South} and ρ_{West}	0.8
ρ_{East} and ρ_{Floor}	0.7
Source	$\mathcal{F}$=$\{(0,0,-2.3);(0,0,1);130\ mW,^{\ddagger}\}$
Receiver	$\mathcal{D}$=$\{(x,y,-2.1);(0,0,1);5\ cm^2, 85°\}$
Number of reflections (N)	5
Δs_1, Δs_2 and $\Delta s_{3,4,5}$	10, 20 and 40 (cm)

Table 1: Room characteristics and main simulation parameters.

Consider a rectangular co-ordinated system with origin at the ceiling centre with axis xx pointing to north, yy pointing to west and zz pointing up at the vertical. South wall has a large green board; east wall contains a large window with a curtain that reflects well IR signals; the others walls are of concrete painted with a brown plastic paint. The ceiling is painted in white and the floor has a brown synthetic cover with a specular reflection pattern. All reflection coefficients were defined based on published values for similar surfaces.[13]

[‡]The source uses an optimised configuration of LEDs as described in the text.

Using a source with all LEDs vertically pointed makes the propagation losses increase rapidly with the emitter to receiver distance, reducing the communication area. Optimisation of the emitter pattern to minimise signal variations allows to increase that area. The optimisation process for this case study resulted in an emitter configuration with: 1 LED ($P_t = 10.0\ mW$ and $hpa = 60°$) vertically oriented, and 8 LEDs ($P_t = 15.0\ mW$ and $hpa = 4.5°$) tilted at 55° with the vertical and uniformly distributed over the azimuth. Two transceivers were implemented according to this configuration, and power distribution over the room space was measured. Figure 3 shows experimental values and simulation results. Simulation results were scaled by 1.16, to equal measured and simulation results at the room

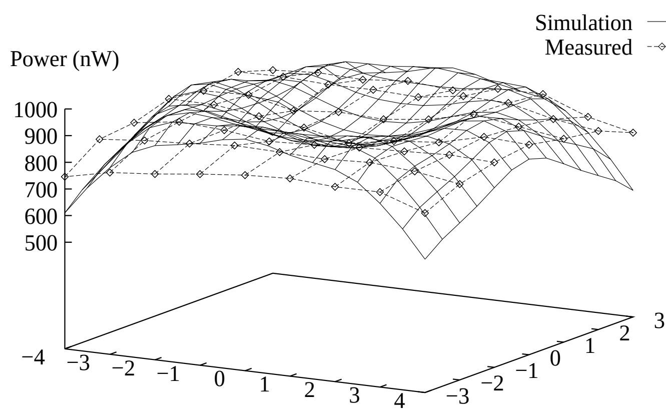

Figure 3: Experimental and simulation results for the power distribution.

centre. This fact is not very relevant as typical values for IR reflection coefficients were considered and LEDs characteristics may change significantly due to the manufacturing process. Apart from the 1.16 factor, it is verified good agreement between experimental values, that vary between 610 and 990 nW, and simulation results, which vary between 756 and 914 nW. Near the room corners there are some differences, where the point source approximation is not fully correct. Simulation results indicate that about 40% of the collected power originate from multiple reflections and that reflections of order 4 and 5 contribute with about 15%, being important to consider them. The good agreement between experimental and simulation results confirm the validity of the approaches implemented in SCOPE. Efficiency of the optimisation process is also confirmed, as when a single lambertian emitter ($P_t = 130.0\ mW$ and $hpa = 60°$) is used, power distribution has an optical range of about 6 dB, and the optimisation process reduced it to less than 1 dB.

4.2 Channel Impulse Response

To validate SCOPE results for the channel impulse response, two diffuse systems will be discussed. In the first system, there is a line-of-sight path between emitter and receiver, while in the second that direct path does not exist. These two channels were already characterised experimentally and simulated,[12] those results are used as reference. Table 2 resumes the channel characteristics, the simulation parameters and the main results obtained. Values used as reference are shown inside parenthesis, which were simulated considering 3 reflections and $\Delta s_1 = 1\ cm$, $\Delta s_2 = 5\ cm$ and $\Delta s_3 = 20\ cm$.

Parameter	Value
Room dimensions ($c \times l \times a$)	$7.5 \times 5.5 \times 3.5\ \ (m)$
$\rho_{Ceiling}$	0.69
ρ_{North}	0.3
ρ_{East}	0.3
ρ_{South}	0.56
ρ_{West}	0.12
ρ_{Floor}	0.09
Source	$\mathcal{F}$=$\{(-1.75, 1.25, -0.2); (0, 0, -1); 1\ W, 60°\}$
Receiver	$\mathcal{D}$=$\{(2.85, 0.05, -2.7); (0, 0, 1); 1\ cm^2, 70°\}$
Number of reflection (N)	3
Δs_1, Δs_2 and $\Delta s_{3,4,5}$	5, 10 and 20 (cm)
Δt	0.2 ns
Line-of-sight collected power	239.1 $nW \rightarrow$ 77.4% (239.1)
1^{st} reflection collected power	18.4 $nW \rightarrow$ 6.0% (18.4)
2^{nd} reflection collected power	41.3 $nW \rightarrow$ 13.4% (39.9)
3^{rd} reflection collected power	9.8 $nW \rightarrow$ 3.2% (9.8)
Total collected power	308.6 nW (307.0)
Channel bandwidth	18.9 MHz (19.5)

Table 2: Main parameters of the diffuse line-of-sight channel.

Figure 4 shows the channel impulse response (subtracted from the line-of-sight delay) considering 3 reflections. Line-of-sight path contributes with a pulse of 239 nW, representing 77.4% of the total collected signal. There is total agreement between SCOPE results and reference values in terms of collected power, channel bandwidth and channel impulse response. Figure 5 shows the channel amplitude response (discrete Fourier transform of the channel impulse response) after 3 and 5 reflections. Considering 3 reflections, the channel bandwidth is 18.9 MHz, while after 5 reflections it is reduced to 16.6 MHz, value that is closer to the 14.0 MHz measured.[12] This reduction results from the signal dispersion that increases significantly with the number of reflections. Reflections 4 and 5 increase the collected power by 5.4 nW and have no influence in the channel transfer function for frequencies above 25 MHz, showing that higher order reflections affect the channel response only at low frequencies. The influence of these reflections would be more significant if IR reflection coefficients were higher. Using a workstation HP 9000C100 with 80 Mbytes of memory, computing time to evaluate the channel impulse response after 1, 2, 3, 4 and 5 reflections was (in minutes): 0.5, 169.2, 262.6, 295.5 e 338.3, respectively. These values show that SCOPE is very time efficient and simulation time increases slowly with the number

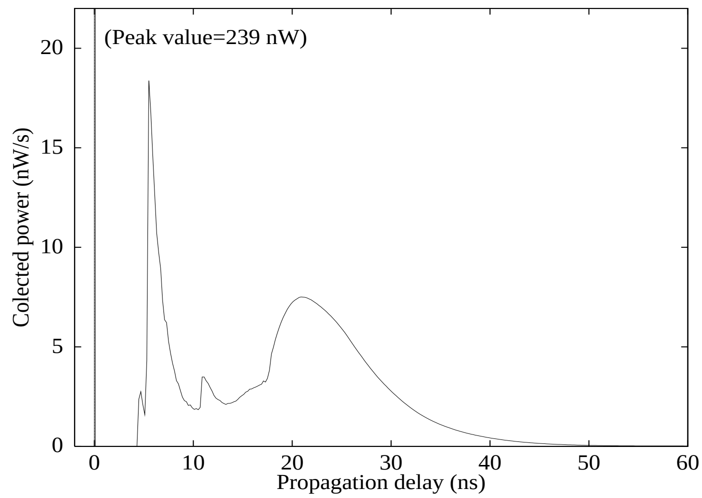

Figure 4: Channel impulse response.

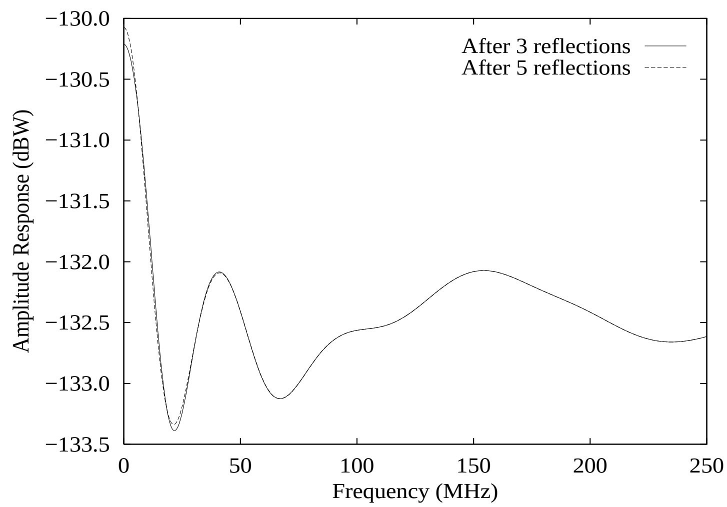

Figure 5: Channel amplitude response after 3 and 5 reflections.

of reflections considered. Computation of $h(t)$ considering 5 reflections required about 15% more time than when considering 4 reflections. These values also show that the spatial resolution affects considerably the simulation time, as computation of $h_2(t)$ ($\Delta s_2 = 10\ cm$) took more time than computation of $h_3(t)$ ($\Delta s_3 = 20\ cm$).

The second channel simulated is a diffuse non line-of-sight configuration, operating in a similar room, but the wall at north has now a reflection coefficient of 0.58. Emitter is at the room centre, 1 m above the floor and is pointed up in the vertical. Receiver is near the floor at the north-east corner of the room and is also pointed up in the vertical. All other channel and simulation parameters are maintained. Table 3 presents channel characteristics, simulation parameters, the main results obtained and, between parenthesis, the values used as reference.[12] Figure 6 shows the channel impulse response considering 3 reflections of the emitted signal. First reflection dominates the channel impulse response, since much

Parameter	Value
Room dimensions ($c \times l \times a$)	$7.5 \times 5.5 \times 3.5 \ (m)$
$\rho_{Ceiling}$	0.69
ρ_{North}	0.58
ρ_{East}	0.3
ρ_{South}	0.56
ρ_{West}	0.12
ρ_{floor}	0.09
Source	$\mathcal{F}$=$\{(0, 0, -2.5); (0, 0, 1); 1\ W, 60°\}$
Receiver	$\mathcal{D}$=$\{(2.25, -1.95, -2.7); (0, 0, 1); 1\ cm^2, 70°\}$
Number of reflections	3
Δs_1, Δs_2 e $\Delta s_{3,4,5}$	5, 10 and 20 (cm)
Δt	0.2 ns
Line-of-sight collected power	0 $nW \rightarrow$ 0% (0.0)
1^{st} reflection collected power	550.0 $nW \rightarrow$ 79.6% (549.8)
2^{nd} reflection collected power	94.3 $nW \rightarrow$ 13.6% (92.4)
3^{rd} reflection collected power	46.7 $nW \rightarrow$ 6.8% (46.9)
Total collected power	691.0 nW (689.8)
Channel bandwidth	31.7 MHz (32.0)

Table 3: Main parameters of the diffuse non line-of-sight channel.

of the collected signal is concentrated near the minimum propagation delay. The channel amplitude response decreases continuously with the frequency, and the channel bandwidth is 31.7 MHz, while the experimental value was 34 MHz. Table 3 shows good agreement between simulation results and reference values, which is also extensible to the channel impulse and frequency responses. When considering 5 reflections, collected power increased to 710.8 nW, while channel bandwidth diminished to 29.4 MHz. Comparing the channel frequency responses after 3 and 5 reflections, we verify that higher order reflections only affect the channel response at frequencies below 30 MHz, and in particular, up to 10 MHz. Computing time are similar to those presented in the previous example.

The results presented for these two channels show good agreement with those already published and verified experimentally. This fact, together with the experimental validation of the power distribution in other simulated channels indicate the SCOPE results are reliable. Using the new algorithm proposed, simulation time increases slowly with the number of reflections. Computation of the channel impulse response considering 5 reflections took less than 6 hours, in contrast with the recursive algorithm, where according to,[12] it would be necessary several years to obtain the channel impulse response considering 5 reflections.

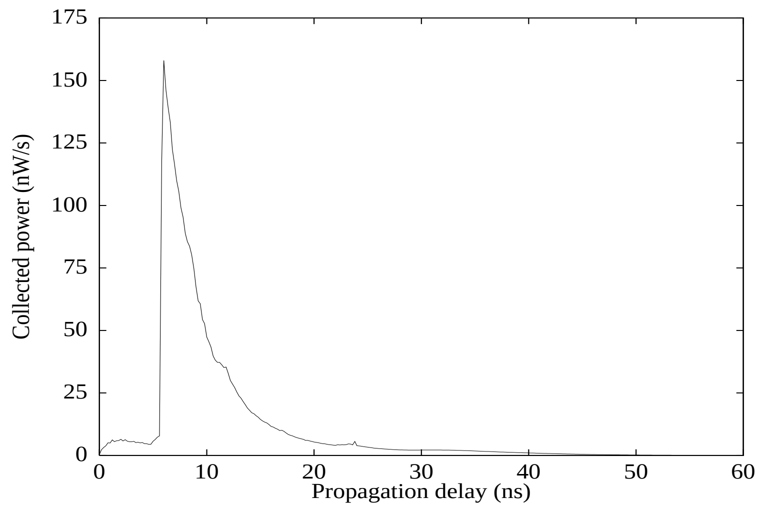

Figure 6: Channel impulse response of the diffuse non line-of-sight channel.

5 Conclusions

A new computationally efficient algorithm for the simulation of indoor wireless optical channels, considering multiple reflections of the emitted signal was proposed. The models used to approximate emitter, reflectors and receiver patterns were reviewed and three propagation models for the simulation of line-of-sight, quasi-diffuse, and diffuse systems were discussed. Two new procedures, called *Time Delay Agglutination* and *Time and Space Indexed Tables*, were proposed to increase time efficiency to obtain the impulse response of indoor wireless optical channels. The new algorithm was implemented in a simulator, called SCOPE, which allows to obtain the main characteristics of indoor optical channels in a time efficient way. Simulation results obtained for a few channels were compared with experimental and published values. The agreement between simulation results and reference values was very good, in terms of collected power, channel bandwidth and channel impulse and frequency responses. Obtained results also show that in some system configurations and indoor environments, simulation of the channel impulse response should consider more than three reflections. Practical results confirm that the computing time of SCOPE increases slowly with the number of reflections considered, making it a time efficient tool for the study of indoor wireless optical channels.

References

[1] C. R. Lomba, R. T. Valadas, and A. M. Duarte. "Combined Emitter and Receiver Diversity to Achieve Data Rates $>$ 100 Mbit/s on Diffuse Optical Channels". *Electronic Letters*, Vol. **34**(12):pp. 1243–1244, June 1998.

[2] D. J. Heatley, D. R. Wisely, Neild I., and P. Cochrane. "Optical Wireless: The Story So Far". *IEEE Communications Magazine*, Vol. **36**(12):pp. 72–82, December 1998.

[3] C. R. Lomba. *"Infrared Wireless Indoor Communications: Modeling, Simulation and Optimisation of the Optical Channel (in Portuguese)"*. PhD thesis, Dept. de Electrónica e Telecomunicações, Universidade de Aveiro, Aveiro, Portugal, May 1997.

[4] J. Kahn and J. Barry. "Wireless Infrared Communications". *Proceedings of the IEEE*, Vol. **85**(2):pp. 265–298, February 1997.

[5] A. C. Moreira. *"Free-Space Optical Transmission Systems for Indoor Environments (in Portuguese)"*. PhD thesis, Dept. de Electrónica e Telecomunicações, Universidade de Aveiro, Aveiro, Portugal, February 1997.

[6] J. R. Barry, J. M. Kahn, E. A. Lee, and D. G. Messerschmitt. "Simulation of Multipath Impulse Response for Indoor Wireless Optical Channels". *IEEE Journal on Selected Areas in Communications*, Vol. **11**(3):pp. 367–379, April 1993.

[7] F. J. Lopez-Hernandez, R. Perez-Jimenez, and A. Santamaria. "Monte Carlo Calculation of Impulse Response on Diffuse IR Wireless Indoor Channels". *Electronic Letters*, Vol. **34**(12):pp. 1260–1262, June 1998.

[8] M. Abtahi and H. Hashemi. "Simulation of Indoor Propagation Channel at Infrared Frequencies in Furnished Office Environments". In *PIMRC'95 – Sixth IEEE International Symposium on Personal, Indoor and Mobile Radio Communications*, pages 306–310, Toronto, Canada, September 1995.

[9] C. R. Lomba, R. T. Valadas, and A. M. Duarte. "Experimental Characterisation and Modelling of the Reflection of Infrared Signals on Indoor Surfaces". *IEE Proceedings on Optoelectronics*, Vol. **145**(3):pp. 191–197, June 1998.

[10] C. R. Lomba. "Simulation of Multipath Impulse Dispersion on Infrared Communication Systems". Technical report, University of Essex, U. K., July 1992.

[11] C. R. Lomba, R. T. Valadas, and A. M. Duarte. "Propagation Losses and Impulse Response of the Indoor Optical Channel: A Simulation Package". In *International Zurich Seminar on Digital Communications*, pages 285–297, Zurich, Switzerland, March 1994. Springer-Verlag.

[12] J. R. Barry. *"Wireless Infrared Communications"*. Kluwer Academic Pub., Boston, USA, 1994.

[13] F. R. Gfeller and U. H. Bapst. "Wireless In–House Data Communications Via Diffuse Infrared Radiation". *Proceedings of the IEEE*, Vol. **67**(11):pp. 1474–1486, November 1979.